Eur. Phys. J. B (2013) 86: 461
DOI: 10.1140/epjb/e2013-40455-x

THE EUROPEAN PHYSICAL JOURNAL B

Regular Article

Fractional kinetic model for granular compaction

S. Živković[1], Z.M. Jakšić[1], J.R. Šćepanović[1], I. Lončarević[2], Lj. Budinski-Petković[2], and S.B. Vrhovac[1,a]

[1] Institute of Physics Belgrade, University of Belgrade, Pregrevica 118, 11080 Zemun, Belgrade, Serbia
[2] Faculty of Engineering, Trg D. Obradovića 6, 21000 Novi Sad, Serbia

Received 1 May 2013 / Received in final form 30 August 2013
Published online 7 November 2013 –

Abstract. We present an approach to granular compaction based on subordination of stochastic processes. In order to imitate, in a very simplified way, the compaction dynamics of granular material under tapping, we impose that particles switch stochastically between the two possible orientational states characterizing the average volumes of the grain in the presence of other grains. The main physical idea of our approach is that the interaction of grains with their environment is taken into account with the aid of the temporal subordination. Accordingly, we assume that the time intervals between the consecutive grain's reorientations are governed by a certain waiting-time distribution $\psi(t)$. It is demonstrated how the presence of the trapping events leads to the macroscopic observation of slow compaction dynamics, described by an exact fractional kinetic equation. We also perform numerical simulations to examine our analytical result. In addition, we reproduce the memory effects numerically by considering the response of the system to the abrupt change in the external excitation.

1 Introduction

Granular compaction describes the phenomenon in which granular materials undergo an increase in the bulk density as a result of the action of external perturbations, such as shaking and periodic shear deformation. A typical density relaxation experiment consists of well-separated accelerations, or taps, of a vertical cylindrical tube holding the granular material. Given that the system relaxes following each tap, reorganization of the grains occurs only during the agitated state. The ability of granular materials to undergo density changes is an inherent property that is not well understood, and thus it remains an open area of research [1].

Different laws have been proposed for the evolution of the volume fraction ρ as a function of the number t of taps. The first experiments on compaction have been carried out by Chicago group for both spherical [2] and anisotropic grains [3]. These experiments have been realized in a long tube with a small diameter comparable with the particle size, giving rise to ordering of the grains near the lateral wall. The compaction dynamics of the strongly confined granular material is described by the inverse logarithmic dependence on the tapping number, $\rho(\infty) - \rho(t) \sim 1/\ln(t)$ [2]. The final density, $\rho(\infty)$, is a monotonic decreasing function of the dimensionless vibration intensity, $\Gamma = A/g$, where A is the peak acceleration in a tap, and g is the gravity. More recently, studies by the Rennes group [4–6] have shown that the compaction dynamics is consistent with the stretched exponential law $\rho(\infty) - \rho(t) \sim \exp[-(t/\tau)^{\alpha}]$. This experiment has been realized in geometrical configuration that allows only negligible wall effects, unlike to the experimental setup of the Chicago group [2,3]. Moreover, in the Rennes group's experiment, convection has been observed in the whole packing, and the compaction dynamics is attributed to a convection mediated mechanism. The corresponding steady state density is suggested to be determined by the dynamical balance between convection and compaction.

Many other experiments have been carried out in quite different systems. Experimental studies of Lumay and Vandewalle [7,8] for two-dimensional granular systems suggested that the slow compaction dynamics is related to the crystallization driven by the diffusion of defects in the packing. Nicolas et al. [9,10] have studied the compaction of a granular assembly of spheres under a periodic shear deformation. They showed that crystalline arrangements are created in the bulk during the compaction, indicating that the order is not wall-induced. They have suggested that when the compaction occurs towards crystallization, previously proposed fits, like inverse logarithmic or stretched exponential function, do not provide a satisfactory description of the time evolution of density. The general conclusion is that different shaking procedures and geometrical constraints give rise to intrinsically different compaction behaviors, driven by different dynamical mechanisms. To the best of our knowledge, there is no consensus concerning the temporal behavior of the density change (see, e.g. Table I in Ref. [8]).

[a] e-mail: vrhovac@ipb.ac.rs

In our previous studies [11,12] we carried out the extensive simulations of the compaction dynamics for a two-dimensional system of frictional mono-sized hard disks, subjected to vertical shaking. We analyzed the compaction dynamics and the microstructural properties of the packing configurations for various values of friction coefficient and coefficient of normal restitution. It was shown that the relaxation behavior of the system strongly depends on the material properties of the grains. Furthermore, we have shown that the compaction dynamics in our simulation is consistent with the Mittag-Leffler law (corresponding mathematical definitions are provided later in the text; see, Eqs. (23)–(25)). Note that the Mittag-Leffler function is one of the most frequently used phenomenological fitting functions for relaxation processes in many complex disordered systems such as glasses, ferroelectric crystals, and dielectrics [13]. It is noticeable that such temporal evolution of the packing fraction shares some similarities with the coverage growth observed in the two-dimensional lattice based reversible random sequential adsorption (RSA) model [14]. The adsorption-desorption model can reproduce qualitatively the densification kinetics [15], memory effects [16,17] and other features of weakly vibrated granular materials. Results of the numerical simulations of reversible RSA on a triangular lattice obtained for a wide variety of object shapes [14] showed an excellent agreement of the relaxation dynamics with the Mittag-Leffler function (Eq. (23)). In addition, we produced a very good Mittag-Leffler fit (23) to the data from the Rennes group's experiment (see Fig. 4 in Ref. [14]).

The same relaxation law (23) was also obtained in the simulation study of compaction by thermal cycling [18,19] in a three-dimensional packed bed using thermal particle dynamics (modified discrete element simulation method). Recently, the role that dilation plays in the granular compaction has been experimentally studied [20]. Confining force was used to limit the amount of dilation of a vertically shaken granular pack. These experiments have shown that the compaction is greatly reduced in the presence of a confining force so that the steady-state regime was inaccessible with this experimental methodology. Since it cannot be found experimentally, the steady-state packing fraction was determined by fitting the compaction behavior to the Mittag-Leffler functional form (23).

It is intriguing that the Mittag-Leffler law (23) has been shown to describe the relaxation of granular materials under very different modes of external excitation. Actually, it is not clear whether equation (23) is just a convenient fitting expression with four parameters or it has a more fundamental meaning, associated to some peculiar dynamical events which are dominant in the density relaxation. We would like to elucidate this point more thoroughly in order to develop a model of granular compaction based on the stochastic fractional process that captures this relaxation dynamics.

A number of different approaches have been proposed in order to connect a very slow compaction of granular materials with the intrinsic properties of granular packings, such as excluded volume effect and presence of cooperative structures (arches or bridges). Most of the studies have been performed for the (off-lattice) reversible adsorption-desorption or parking lot model [15,21,22], frustrated lattice gas models [23–26], cellular-automaton models [27] and one-dimensional lattice models with short-range dynamical constraints [28–31]. Here we imagine an artificial, but instructive model of a powder similar to the "two-volume" model proposed by Edwards and Grinev [32]. We suppose that there are only two possible configurations of grains. Grain in the "down" state is "well oriented", which means that the surrounding void space is minimal; conversely, when the grain is in the "up" state, or "not well oriented", the free volume is maximal. In order to imitate, in a very simplified way, the compaction dynamics of a granular material under weak tapping, we impose that the particles switch stochastically between the two orientational states. By appropriately choosing this random process, one can provide the essential ingredients in our model to reproduce the slow compaction dynamics and memory effects [9,33].

During the external tapping of real granular materials, a rearrangement will occur between those grains in the packing whose configuration and neighbors produce a force which is overcome by the external disturbance. The magnitude of the forces between particles in contact and their confinement determine whether the particle will move or not. This implies that there are regions in the sample in which the contact network changes and those which are unperturbed. For example, mutually stabilized sets of particles, such as arches or bridges are long-lived during the tapping [11,34–36]. Furthermore, the particle motion observed during the compaction is not diffusive, but exhibits a transient cage effect. The cage changes involve complex cooperative processes associated with modifications in the force network [10,37]. Such properties of the individual motion of the grains may be related to the non-Markovian nature of the stochastic process present in the granular packing submitted to tapping.

Starting with the description of the two-state system evolution as a Markovian process, we develop the analysis on subordinated random process. The process differs from the Markovian ones by the temporal variable becoming random. The subordination of a random process is a starting point for the continuous time random walk approach (CTRW) [38]. Actually, in our model the evolutions of the number of objects in the states "up" and "down" are subordinated by another random process. Recall that a subordinated process $Y[U(t)]$ is obtained by randomizing the time clock of a random process $Y(t)$ using a random process $U(t)$. The latter process is referred to as the randomized time. The new clock generalizes the deterministic time clock of the kinetic equation for the Markovian process. This generalization is of a stochastic origin and produces the fractional operator in the resulting evolution equation of density, i.e. the inclusion of memory. The evolution equation is capable of reproducing a wide range of known experimental behavior. We think that the success of the model in emulating the experiments indicates that the dominant physical mechanisms have been correctly

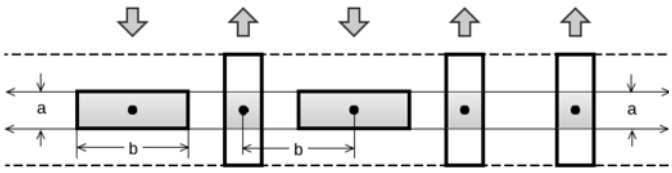

Fig. 1. Schematic picture of the compaction model described in the text.

identified. Even though the model is simple enough as to be analytically tractable, the theoretical results are corroborated by numerical simulations of the corresponding stochastic fractional processes.

The layout of this work is organized as follows. Definition of the model and discussion on the physical interpretation of the model parameters are given in Section 2. In Section 3 results of numerical simulation are presented, discussed, and wherever possible compared with analytical results. In addition, we reproduce the memory effects numerically by considering the response of the system to the abrupt change in the external excitation. Finally, we summarize our findings in Section 4.

2 The model and its properties

We consider a one-dimensional lattice of width bN ($b > 0$), with N noninteracting "grains" located at its lattice points. Each "grain" is a rectangle with sides a and b ($a < b$), whose midpoint is located at a grid site. They can take two possible orientations, referred to as *down* ("well oriented") and *up* ("not well oriented"). Our one-dimensional lattice model can be regarded as a very simple picture of a horizontal section of a real granular system (see Fig. 1). Horizontally aligned grains ("well oriented") result in a fully packed section of height a. Vertical orientations generate voids; each "not well oriented" grain leaves a void of size $v_0 = a(b - a)$ in the horizontal section of height a (Fig. 1). A configuration of the system is uniquely defined by N orientation variables $\{\sigma_n | n = 1, \ldots, N\}$, with $\sigma = +1$ denoting a horizontal grain, and $\sigma = -1$ denoting a vertical grain.

The phenomenon of compaction results from the existence of packing defects, such as voids, in a randomly packed granular material. Physically, a major mechanism of compaction of weakly vibrated granular materials is the gradual collapse of long-lived bridges, resulting in the disappearance of the void space which is trapped in the arches ("bridge collapse") [34,36,39]. Shaking of the material causes rearrangement of grains and interstitial voids, and the granular material "jumps" between different, but related, grain configurations. The dynamic response of the granular system to forcing excitation is such as to minimize the void space locally. This can be accomplished in the model by means of the elimination of holes.

From the phenomenological point of view, we can try to model the above, naively, by a continuous-time stochastic dynamics, described by the following general kinetic equations:

$$\frac{dp^{(\mathrm{d})}}{dt} = \omega_{\mathrm{du}} p^{(\mathrm{u})}(t) - \omega_{\mathrm{ud}} p^{(\mathrm{d})}(t) \tag{1}$$

$$\frac{dp^{(\mathrm{u})}}{dt} = \omega_{\mathrm{ud}} p^{(\mathrm{d})}(t) - \omega_{\mathrm{du}} p^{(\mathrm{u})}(t), \tag{2}$$

where $p^{(\mathrm{u})}(t)$ and $p^{(\mathrm{d})}(t)$ are the probabilities for finding the object in the states "up" and "down" at time t, respectively. Here ω_{du} and ω_{ud} represent, respectively, the constant transition probability rate from the state "up" to the state "down", and from the state "down" to the state "up". The term $\omega_{\mathrm{du}} p^{(\mathrm{u})}$ describes transition into the state "down" from state "up", and $\omega_{\mathrm{ud}} p^{(\mathrm{d})}$ corresponds to transition out of the "down" into the other state "up". Thus we write the packing fraction $\rho(t)$ as:

$$\begin{aligned} \rho(t) &= \rho_d p^{(\mathrm{d})}(t) + \rho_{\mathrm{u}} p^{(\mathrm{u})}(t) \\ &= \rho_{\mathrm{u}} + (\rho_d - \rho_{\mathrm{u}}) p^{(\mathrm{d})}(t). \end{aligned} \tag{3}$$

We have two limits: $p^{(\mathrm{d})} = 1$ when $\rho = \rho_d$ (free volume is minimal), and $p^{(\mathrm{d})} = 0$ when $\rho = \rho_{\mathrm{u}}$ (free volume is maximal). Without loss of generality we assume that $\rho_d = 1$ and $\rho_{\mathrm{u}} = a/b < 1$ in our model. Setting $\left.\frac{dp^{(\mathrm{d})}}{dt}\right|_{t\to\infty} = 0$ and $\left.\frac{dp^{(\mathrm{u})}}{dt}\right|_{t\to\infty} = 0$ in equations (1) and (2) they become a set of two algebraic equations whose solution provides the steady-state values of the packing fraction $\rho(\infty)$:

$$\rho(\infty) = \rho_{\mathrm{d}} p^{(\mathrm{d})}(\infty) + \rho_{\mathrm{u}} p^{(\mathrm{u})}(\infty) = (\rho_{\mathrm{d}} \omega_{\mathrm{du}} + \rho_{\mathrm{u}} \omega_{\mathrm{ud}})/\omega, \tag{4}$$

where $\omega = \omega_{\mathrm{du}} + \omega_{\mathrm{ud}}$ is the total transition probability rate. This steady state will be reached by the system from any initial configuration. Assume that for $t = 0$ the states "up" dominate, i.e.

$$p^{(\mathrm{u})}(0) = \frac{N_{\mathrm{u}}(t=0)}{N} = 1, \quad p^{(\mathrm{d})}(0) = \frac{N_{\mathrm{d}}(t=0)}{N} = 0, \tag{5}$$

where N_{u} and N_{d} are the number of objects in the states "up" and "down", respectively. The solution of equations (1) and (2) with initial conditions (5) is straightforward. Accordingly, the packing fraction of the system (Eq. (3)) grows exponentially in time towards the steady state value:

$$\rho(t) = \rho(\infty) - [\rho(\infty) - \rho(0)] \exp(-\omega t), \tag{6}$$

where $\rho(0) = \rho_{\mathrm{d}} p^{(\mathrm{d})}(0) + \rho_{\mathrm{u}} p^{(\mathrm{u})}(0) = \rho_{\mathrm{u}}$. Not unexpectedly, our simplified model does not describe the behavior of a real granular material during the compaction appropriately; i.e., it is not a good approximation for the compaction dynamics. Furthermore, in the present model the future evolution of the packing fraction $\rho(t)$ after time t_0 depends only on $\rho(t_0)$. However, the behaviour of a weakly vibrated granular material depends on its entire tapping history, and not only on the instantaneous, initial value of the property under study. Mathematically, this phenomenon implies that the time evolution of the packing fraction does not obey a closed system of first-order ordinary differential equations.

Our model requires substantial addition and extension in order to have the ability to properly capture the dynamics of compaction and memory effects observed for a discontinuous shift in tapping intensity. Before we make a step further in the modeling, several important facts should be mentioned about the structural transformations of the granular packing during the compaction. One of the most distinctive features in the structure of granular packings is the presence of arches or bridges [34,36,39]. An arch is a set of particles such that we can trace a path of connected particles between any pair in the set [34]. A great number of particles are involved in such structures. Arches are responsible for the voids that determine the volume fraction of packing [39]. This multi-particle structure is stable thanks to the contributions of every particle in it. Should any particle of the bridge be removed, the entire bridge would collapse under gravity. During the tapping, the grains in the bulk experience the external perturbation as a random force. The grains have some freedom to rearrange their positions relative to their neighbors. Therefore, the change of a certain configuration occurs due to the cooperative rearrangement of free volume between the neighboring grains. If the intensity of vibration is sufficiently small, some grains are not able to break away from their clusters, so structures such as bridges are long-standing even during tapping. A bridge, once being formed, usually lasts during a great number of taps [11]. Hence, during the compaction the grains spend most of the time trapped in localized regions or "cages" and occasionally exhibit longer displacements [10,37,40]. As the packing progressively densifies, the time which grains spend in a cage becomes longer and longer and the grains move around a fixed position. The relaxation process in such dense systems is characterized by the temporally nonlocal behavior arising from the disorder which produces obstacles or traps which delay the motion of the particles and introduce memory effects into the motion. The main physical idea of our approach is that the time intervals between the consecutive grain's reorientations are governed by a certain waiting-time distribution $\psi(t)$. That function governs the *random time* intervals between single microscopic jumps ("up" $\leftrightarrow$ "down") of the particles.

Assume that the interaction of grains with their environment is taken into account with the aid of subordination in time. We shall consider the evolution of the number of objects in the states "up" and "down". These are *parent* random processes in the sense of subordination. Consider a sequence T_i, $i = 1, 2, \ldots$ of non-negative, independent, identically distributed random variables which represent the waiting time intervals between consecutive reorientations of objects. If the waiting times T_i belong to the strict domain of attraction of an α-stable distribution ($0 < \alpha < 1$), their sum $n^{-1/\alpha}\sum_{i=1}^{n} T_i$, $n \in \mathrm{N}$ converges in distribution to a stable law with the same index α [41,42]. The continuous limit of the discrete counting process $\{N_t\}_{t\geq 0} = \max\{n \in \mathrm{N} | \sum_{i=1}^{n} T_i \leq t\}$ is the hitting time process $S(t)$ (also called the first passage time). We choose the nondecreasing random process $S(t)$ for a new time clock (stochastic time arrow). The probability density of the process $S(t)$ has the following form [43]:

$$p_\alpha^S(t,\tau) = \frac{1}{2\pi j}\int_{\mathrm{Br}} u^{\alpha-1}\exp(ut-\tau u^\alpha)\mathrm{d}u = t^{-\alpha}F_\alpha\left(\frac{\tau}{t^\alpha}\right), \tag{7}$$

where Br denotes the Bromwich path and $j = \sqrt{-1}$. The function $F_\alpha(z)$ can be expanded as a Taylor series:

$$F_\alpha(z) = \sum_{k=0}^{\infty}\frac{(-z)^k}{k!\,\Gamma(1-\alpha-k\alpha)}, \tag{8}$$

where $\Gamma(\cdot)$ is the gamma function. The probability density $p_\alpha^S(t,\tau)$ determines the probability to be at the internal time (or so-called operational time) τ on the real time t [44].

The stochastic time arrow can be applied to the kinetic equations (1) and (2). Take the process $S(t)$ as a subordinator. It accounts for the amount of time when an object does not change its orientation. If $p^{(\mathrm{d})}(\tau)$ and $p^{(\mathrm{u})}(\tau)$, taken from equations (1) and (2) as probability laws of the parent process, depend now on the local time τ, then the resulting probabilities $p_\alpha^{(\mathrm{d})}(t)$ and $p_\alpha^{(\mathrm{u})}(t)$ after the subordination are determined by the integral relations:

$$p_\alpha^{(\mathrm{d})}(t) = \int_0^\infty d\tau\; p_\alpha^S(t,\tau)p^{(\mathrm{d})}(\tau) \tag{9}$$

$$p_\alpha^{(\mathrm{u})}(t) = \int_0^\infty d\tau\; p_\alpha^S(t,\tau)p^{(\mathrm{u})}(\tau). \tag{10}$$

Now the compaction of the system is defined by two stochastic processes, random waiting times between random reorientations. The ratio of objects in the state "up" and another in the state "down" is subordinated by the process $S(t)$. In other words, the compaction process (Eqs. (9) and (10)) is obtained by randomizing the time clock of the continuous-time stochastic dynamics (Eqs. (1) and (2)) using the random process $S(t)$ [44].

The equation describing the present model takes the form similar to equations (1) and (2), but the derivatives of first order become fractional of order $0 < \alpha < 1$ determined by the index of the process $S(t)$. Let us present equations (1) and (2) in compact form:

$$\frac{d}{dt}\boldsymbol{p}(t) = \hat{\boldsymbol{\omega}}\,\boldsymbol{p}(t), \tag{11}$$

where $\boldsymbol{p}(t) = \left[p^{(\mathrm{d})}(t)\; p^{(\mathrm{u})}(t)\right]^T$, and $\hat{\boldsymbol{\omega}}$ denotes the transition rate operator:

$$\hat{\boldsymbol{\omega}} = \begin{bmatrix} -\omega_{\mathrm{ud}} & \omega_{\mathrm{du}} \\ \omega_{\mathrm{ud}} & -\omega_{\mathrm{du}} \end{bmatrix}. \tag{12}$$

It is important to note that the operator $\hat{\boldsymbol{\omega}}$ is independent of time. Equation (11) can be written in the integral form

$$\boldsymbol{p}(t) = \boldsymbol{p}(0) + \int_0^\infty d\tau\;\hat{\boldsymbol{\omega}}\,\boldsymbol{p}(\tau). \tag{13}$$

The Laplace transform of equation (13) gives the relation

$$\hat{\boldsymbol{\omega}}\,\tilde{\boldsymbol{p}}(s) = s\tilde{\boldsymbol{p}}(s) - \tilde{\boldsymbol{p}}(0), \tag{14}$$

where the Laplace transform $\mathcal{L}$ is defined as:

$$\mathcal{L}\boldsymbol{p}(t) \equiv \tilde{\boldsymbol{p}}(s) = \int_0^\infty dt \exp(-st)\boldsymbol{p}(t). \tag{15}$$

In the Laplace space the probabilities $\boldsymbol{p}_\alpha(t) = \left[p_\alpha^{(\mathrm{d})}(t)\ p_\alpha^{(\mathrm{u})}(t)\right]^T$ (see, Eqs. (9) and (10)) take the most simple form

$$\tilde{\boldsymbol{p}}_\alpha(s) = s^{\alpha-1}\tilde{\boldsymbol{p}}(s^\alpha), \tag{16}$$

since $\tilde{p}_\alpha^S(s,\tau) = s^{\alpha-1}\exp(-\tau s^\alpha)$ [45]. When operator $\hat{\boldsymbol{\omega}}$ acts on the Laplace image $\tilde{\boldsymbol{p}}_\alpha(s)$ (Eq. (16)), we obtain

$$\begin{aligned}\hat{\boldsymbol{\omega}}\tilde{\boldsymbol{p}}_\alpha(s) &= s^{\alpha-1}\hat{\boldsymbol{\omega}}\tilde{\boldsymbol{p}}(s^\alpha) = s^{\alpha-1}\left(s^\alpha\tilde{\boldsymbol{p}}(s^\alpha) - \tilde{\boldsymbol{p}}(0)\right)\\ &= s^\alpha\tilde{\boldsymbol{p}}_\alpha(s) - s^{\alpha-1}\tilde{\boldsymbol{p}}(0).\end{aligned} \tag{17}$$

The inverse Laplace transform $\mathcal{L}^{-1}$ of the latter expression (17) gives the abstract partial differential equation with the fractional derivative of time:

$$\boldsymbol{p}_\alpha(t) = \boldsymbol{p}(0) + {}_0D_t^{-\alpha}\hat{\boldsymbol{\omega}}\,\boldsymbol{p}_\alpha(t). \tag{18}$$

Here we use the fractional Riemann-Liouville integral operator defined via the formula

$${}_0D_t^{-\alpha}f(t) = \frac{1}{\Gamma(\alpha)}\int_0^t d\tau\ (t-\tau)^{\alpha-1}f(\tau), \quad 0<\alpha<1, \tag{19}$$

with the convenient property $\mathcal{L}[{}_0D_t^{-\alpha}f(t)] = s^{-\alpha}\tilde{f}(s)$ [46]. Using equation (18) and taking into account that $\rho(t) = \rho_d p_\alpha^{(\mathrm{d})}(t) + \rho_\mathrm{u} p_\alpha^{(\mathrm{u})}(t)$, we obtain that the deviation $\Delta\rho(t) = \rho(\infty) - \rho(t)$ of the packing fraction $\rho(t)$ from its steady-state value $\rho(\infty)$ obeys the fractional differential equation

$$\Delta\rho(t) = \Delta\rho(0) - \omega\left[{}_0D_t^{-\alpha}\Delta\rho(t)\right], \tag{20}$$

where $\omega = \omega_\mathrm{du} + \omega_\mathrm{ud}$ is the total transition probability rate and $\rho(\infty)$ is defined by equation (4). In equation (20), the fractional derivative on the r.h.s. describes a process which is subordinated to the simple orientational switching; the subordination is defined by the α-stable waiting time distribution. By differentiating equation (20) with respect to time and with the help of the formula [46]

$$\frac{d}{dt}\,{}_0D_t^{-\alpha}f(t) = {}_0D_t^{1-\alpha}f(t), \tag{21}$$

it is found that

$$\frac{d}{dt}\Delta\rho(t) = -\tau_r^{-\alpha}\,{}_0D_t^{1-\alpha}\Delta\rho(t), \tag{22}$$

where $\tau_r = \omega^{-1/\alpha}$. Equation (22) is an integro-differential equation. The Riemann-Liouville operator ${}_0D_t^{1-\alpha}$ introduces a convolution integral with the power-law kernel $M(t) \propto t^{\alpha-2}$. Therefore, the fractional equation (22) involves a slowly decaying memory, so the present packing fraction $\rho(t)$ of the system depends strongly on its history $\rho(t')$, $t' < t$. This is in accordance with the fact that granular materials are intrinsically non-local in time [1].

The parameter τ_r may be interpreted as a generalized relaxation time. Indeed, the solution of equation (22) can be expressed in terms of the Mittag-Leffler function E_α of order α via [46,47]

$$\Delta\rho(t) = \Delta\rho(0)E_\alpha\left[-\left(\frac{t}{\tau_r}\right)^\alpha\right]. \tag{23}$$

Mittag-Leffler function is defined by the following inverse Laplace transform:

$$E_\alpha\left[-(t/\tau)^\alpha\right] = \mathcal{L}^{-1}\left\{(u+\tau^{-\alpha}u^{1-\alpha})^{-1}\right\}, \tag{24}$$

from which the series expansion

$$E_\alpha\left[-(t/\tau)^\alpha\right] = \sum_{n=0}^\infty \frac{(-(t/\tau)^\alpha)^n}{\Gamma(1+\alpha n)} \tag{25}$$

can be deduced [47].

Two important questions are still not answered. First, the model just outlined is incomplete as it does not incorporate the experimentally controlled parameter Γ. Mapping the model on to the experiment, "up"→"down" event is associated with the annihilation or filling of a void within the horizontal section, whereas a "down"→"up" event is associated with the creation of a void. The crucial parameter which determines the final steady-state packing fraction $\rho(\infty)$ and controls the dynamics, is the ratio $\gamma = \omega_\mathrm{ud}/\omega_\mathrm{du}$ and within a model plays a role similar to that of the intensity of vibration Γ in real experiments. According to equation (4), the steady-state value of the packing-fraction $\rho(\infty)$ is determined by:

$$\rho(\infty) = \frac{\rho_d + \rho_\mathrm{u}\gamma}{1+\gamma}. \tag{26}$$

The packing fraction $\rho(\infty)$ is a decreasing function of the parameter $\gamma \geq 0$ and varies between $\rho_\mathrm{u} = a/b$ $(\gamma \to \infty)$ and $\rho_d \leq 1 (\gamma = 0)$.

Second, it is important to note that the coefficient α is not independent as far as its functional dependence on the "tapping intensity" γ is concerned. We postulate that parameters $0 < \alpha < 1$ and $\gamma > 0$ obey a simple relation:

$$\alpha = \frac{1}{1+1/\gamma}. \tag{27}$$

The value of parameter α increases monotonically toward unity as a function of the "tapping intensity" γ. This relationship can be justified by the following phenomenological argument. Since the waiting-time intervals T_i belong to an α-stable distribution $(0 < \alpha < 1)$, the probability that T_i is greater than some number $t > 0$ (tail probability) is asymptotically power law, i.e. $P(T_i > t) \propto t^{-\alpha}$ as $t \to \infty$ [41]. Accordingly, decreasing of the parameter α in the range $(0, 1)$ increases the contribution of long waiting-time intervals T_i during the compaction process. This is in accordance with the fact that during the low-intensity tapping some cooperative structures in the packing are long-standing, while for the high-intensity tapping regime,

cooperative structures form and disappear rapidly. Analogously, in the present model, "up" and "down" states are preserved for longer times for the lower tap intensities. It is important to notice that the "tapping intensity" γ influences the compaction dynamics indirectly through the parameter α (Eq. (27)). But, the parameter α does not affect the value of the steady-state packing fraction $\rho(\infty)$. Furthermore, in the next section by virtue of equation (27) it will be shown that the relaxation time τ_r versus γ follows an Arrhenius behavior $\tau_r \propto \exp(\gamma_0/\gamma)$ [5]. Note that Arrhenius-like forms have already been reported in some previous studies on the granular compaction under tapping [1,4,48,49]. Such a relaxation law is also found for strong glasses. The Arrhenius-like process describes the escape probability of a thermally or mechanically activated particle from a potential well. In granular systems, thermal effects are negligible, and we hypothesize that the mechanical excitation plays the role of a thermal energy source.

3 Numerical simulation and results

Here we compare the theoretical predictions described in the previous section with the results of the numerical simulations of the present compaction model. The numerical simulations are based on the numerical algorithm for the simulation of fractional Fokker-Plank dynamics described in more detail in references [50,51]. Let us briefly describe the algorithm used in our numerical simulation.

At each Monte Carlo step one lattice site is selected at random, and one of the two possible transitions between the two different states of the object is chosen at random. The choice of the transition from the state "up" to the state "down" occurs with probability $p_{\rm du}$, and from the state "down" to the state "up" with probability $p_{\rm ud}$. The transition probabilities obey the normalization condition $p_{\rm du}+p_{\rm ud}=1$, and determine the "tapping intensity" γ. When the attempted process is an "up" $\rightarrow$ "down" transition, and if randomly chosen object is in the "up" state, its state switches form "up" to "down". On the contrary, if randomly chosen object is in the "down" state the attempt is abandoned. When the attempted process is a "down" $\rightarrow$ "up" transition, and provided that the selected object is in the "down" state, the object state is changed from the "down" to "up". Otherwise, we reject the reorientation trial. Reorientation processes are assumed to happen instantaneously or at least in negligible time. The random time τ between two reorientation attempts is extracted from a residence time distribution $\psi(\tau)$. A suitable possible choice for $\psi(\tau)$ is a Mittag-Leffler distribution defined by:

$$\psi(\tau) = -\frac{d}{d\tau} E_\alpha(-(\tau/\nu)^\alpha), \tag{28}$$

where the constant ν is the time-scaling parameter, and the parameter α is determined by relation (27). The basic role of the Mittag-Leffler waiting time probability density in the time fractional continuous time random walk (CTRW) has become well known by the seminal paper of Hilfer and Anton [52]. Fulger et al. [53] paid special attention to its use as a waiting time law in the CTRW simulation. The probability density $\psi(\tau)$ for the waiting times can be numerically calculated by series expansion (25). This method produces a pointwise representation of the density on a finite interval. Random numbers can then be produced by rejection, most efficiently with a look-up table and interpolation. More convenient is the following inversion formula by Kozubowski and Rachev [54]:

$$\tau = -\nu \ln u \left(\frac{\sin(\alpha\pi)}{\tan(\alpha\pi v)} - \cos(\alpha\pi) \right)^{1/\alpha}, \tag{29}$$

where $u, v \in (0,1)$ are independent uniform random numbers, ν is the scale parameter, and τ is a Mittag-Leffler random number. For $\alpha = 1$, equation (29) reduces to the inversion formula for the exponential distribution, i.e. $\tau = -\nu \ln u$. In each computational step the time t and the packing fraction ρ are updated, $t \rightarrow t+\tau$ and $\rho \rightarrow \rho + \Delta\rho$, where $\Delta\rho \in \{\pm(1-a/b)/N, 0\}$. Reiterating this algorithm, the full density growth above the initial packing fraction $\rho(0) = \rho_{\rm u} = a/b$ to the steady-state limit $\rho(\infty)$ (Eq. (4)) can be computed.

The time-scaling parameter ν in equation (29) is calculated using the procedure detailed in references [50,51]. The quantities $\omega_{\rm du} = (p_{\rm du}/N)\nu^{-\alpha}$ and $\omega_{\rm ud} = (p_{\rm ud}/N)\nu^{-\alpha}$ in the fractional kinetic equation (20) are referred to as the fractional "up" $\rightarrow$ "down" and "down" $\rightarrow$ "up" rates. Using the normalization condition for the transition probabilities, i.e. $p_{\rm du} + p_{\rm ud} = 1$, one obtains that:

$$p_{\rm du} = \frac{\omega_{\rm du}}{\omega_{\rm du}+\omega_{\rm ud}}, \quad p_{\rm ud} = \frac{\omega_{\rm ud}}{\omega_{\rm du}+\omega_{\rm ud}}, \tag{30}$$

and

$$\nu = (N(\omega_{\rm du}+\omega_{\rm ud}))^{-1/\alpha}. \tag{31}$$

In that case, the results of simulations are independent of the number of objects in the system. The fractional rates can be chosen as:

$$\omega_{\rm du} = \omega\frac{1}{1+\gamma}, \quad \omega_{\rm ud} = \omega\frac{\gamma}{1+\gamma}, \tag{32}$$

where $\gamma = p_{\rm ud}/p_{\rm du}$. We impose that parameter $\omega > 0$ in equation (32) depends only on the micromechanical properties of the granular system. In fact, the form (32) of the fractional rates ensures that the total rate $\omega_{\rm du}+\omega_{\rm ud} = \omega \neq f(\gamma)$ is independent on the tapping intensity γ.

All numerical simulations were performed on a system of $N = 100$ rectangles with aspect ratio $a/b = 1/3$; moreover, the parameter ω was chosen as $\omega = 10^{-2}$, so that $\nu = 1$. Figure 2 shows a single realization of the temporal evolution of the packing fraction $\rho(t)$ for two values of "tapping intensity", $\gamma = 2/3$ ($\alpha = 0.4$) and $\gamma = 3/2$ ($\alpha = 0.6$). Obviously, with smaller γ (or, equivalently, with smaller α) the waiting times become longer. Similar curves are obtained with different values of γ.

In order to sufficiently diminish statistical fluctuations, it is necessary to average over many independent runs for each value of the parameter γ. Therefore, curves of the

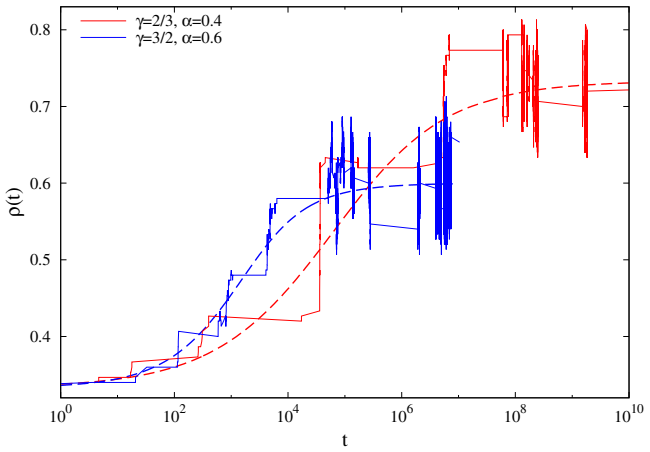

Fig. 2. A single realization of the temporal evolution of the packing fraction $\rho(t)$ for two values of tapping intensity, $\gamma = 2/3$ ($\alpha = 0.4$) and $\gamma = 3/2$ ($\alpha = 0.6$). The dashed lines show the Mittag-Leffler behavior (Eq. (23)), and serve as a guide to the eye.

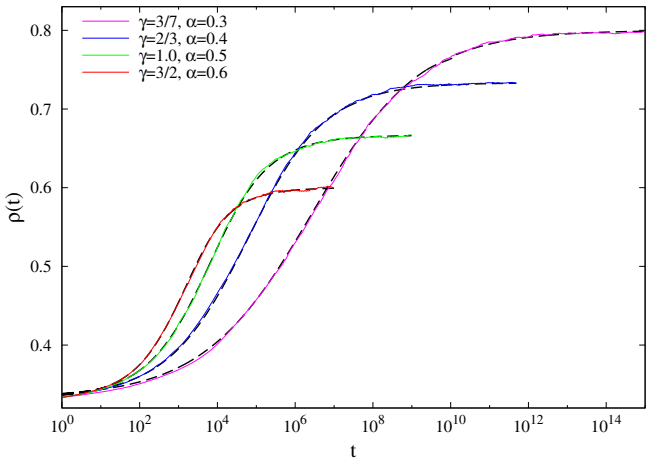

Fig. 3. Temporal evolution of the packing fraction $\rho(t)$ obtained through Monte-Carlo simulations (solid lines) and analytically (dashed lines) for various tapping intensities $\gamma = 3/7,\ 2/3,\ 1,\ 3/2$.

density relaxation reported here are averages of $K = 1000$ independent simulations. To compute the average packing fraction, we introduce a time array $t_m = t_f^{(m-1)/M}$, $m = 1, 2, \ldots, M+1$, where t_f is the final time, and $\log t_{m+1} - \log t_m = \log t_f/M = \text{const}$. Each density curve $\rho^{(k)}(t)$, $k = 1, \ldots, K$ is separately evolved with time, until the final time t_f is reached, $t \geq t_f$. As the kth density curve $\rho^{(k)}(t)$ reaches a measurement time t_m, the packing fraction $\rho^{(k)}(t_m)$ will be computed as a mean value of the packing fractions $\{\rho^{(k)}(t)|t_m \leq t \leq t_{m+1}\}$. Then, all corresponding packing fractions $\rho^{(k)}(t_m)$, $m = 1, 2, \ldots, M+1$ will be saved for this kth run. After evolving all the K density curves $\rho^{(k)}(t)$, the average packing fraction $\rho(t_m)$ at the fixed time t_m is computed by normalization $\rho(t_m) = \sum_{k=1}^{K} \rho^{(k)}(t_m)/K$.

Now, we present and discuss results regarding the temporal evolution of the packing fraction $\rho(t)$. The variation of the packing fraction $\rho(t)$ with time for several tapping intensities γ is presented in Figure 3. The simulation curves are in good qualitative agreement with the experimental data obtained in experiments with a reduced lateral confinement [4,5]. We have observed that the compaction dynamics gets slower when the tapping intensity γ decreases. Actually, when a small tapping intensity is applied, the evolution of the packing fraction toward the steady-state value $\rho(\infty)$ takes place on much wider time scale and finally a larger value of the asymptotic packing fraction is achieved. In the same figure, the relaxation curves obtained analytically by equation (23) are also given, demonstrating that the Mittag-Leffler law (23) is excellently obeyed in our simulations. For large values of γ, there is a rapid approach to the steady-state density $\rho(\infty)$, and consequently the parameter α reaches a value close to 1 (see Eq. (27)). Since $E_\alpha[-(t/\tau_r)^\alpha] \to \exp(-t/\tau_r)$ when $\alpha \to 1$, the slow ("glassy") relaxation feature disappears in the regime of strong tapping intensities.

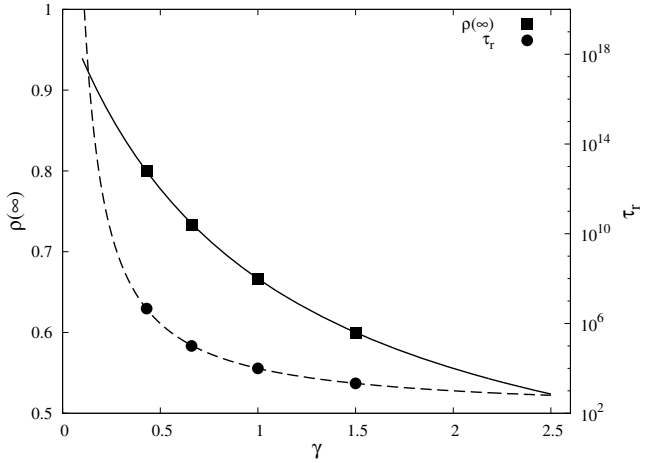

Fig. 4. The steady-state packing fraction $\rho(\infty)$ and the generalized relaxation time τ_r, as functions of the tapping intensity γ. Squares are the simulation results for $\rho(\infty)$ at $\gamma = 3/7,\ 2/3,\ 1,\ 3/2$. Circles are the corresponding values of the relaxation time, $\tau_r \equiv \omega^{-1/\alpha} = 4.64 \times 10^6,\ 10^5,\ 10^4,\ 2.15 \times 10^3$. The descending solid curve (left axis) shows the analytic relation between the steady-state packing fraction $\rho(\infty)$ and γ (see Eq. (26)). The dashed superimposed line (right axis) corresponds to the Arrhenius law $\tau_r \propto \exp(\gamma_0/\gamma)$, where $\gamma_0 = \ln(1/\omega) \approx 4.6$.

In Figure 4 the values of the steady-state packing fraction $\rho(\infty)$ versus the control parameter γ are reported for the simulation results shown in Figure 3. As it can be seen, the decrease of the steady-state packing fraction $\rho(\infty)$ follows an algebraic dependence (26). In addition, we have carried out the annealing procedure analog to the experiment described in [55,56]: the tapping intensity is continuously increased, then decreased, and increased again. Using our model and the same protocol, we only recover the reversible branch which coincides with the solid line in Figure 4. The steady-state density only

depends on the tapping intensity and not on the initial conditions. This can be explained by the fact that the number of taps used in simulations is large enough to allow our system to reach stationarity. The absence of irreversible branch was also observed in the Rennes group's experiments on granular compaction [6]. Thus, aging and irreversible-reversible behaviors are observed only when the steady-state is not reached.

Also, the values of the generalized relaxation time $\tau_r = \omega^{-1/\alpha}$ for $\gamma = 3/7,\ 2/3,\ 1,\ 3/2$ are given in Figure 4. Using the values $\gamma_0 = \ln(1/\omega)$ and $\tau_0 = 1/\omega$, we plot the Arrhenius law

$$\tau_r = \tau_0 \exp(\gamma_0/\gamma), \tag{33}$$

as the dashed curve in Figure 4. In fact, the decay of τ_r with γ can be accurately described by the Arrhenius law (33). Indeed, inserting expressions $\gamma_0 = \ln(1/\omega) \neq f(\gamma)$ and $\tau_0 = 1/\omega \neq f(\gamma)$ into equation (33), and eliminating γ with the help of the relation (27), we can obtain the expression for the generalized relaxation time, $\tau_r = \omega^{-1/\alpha}$ (see Eq. (22)).

Memory effects

In this subsection we focus on the response of the present model to sudden perturbation of the tapping intensity γ. In the compaction experiment [9,33], the tapping intensity (or the shear amplitude) was instantaneously changed from a value Γ_1 to another Γ_2 at a given time t_w. For a sudden decrease in Γ ($\Gamma_1 > \Gamma_2$) it was observed that on short-time scales the compaction rate increases, while for a sudden increase in Γ ($\Gamma_1 < \Gamma_2$) the system dilates for short times. This behavior is transient, and after several taps the usual compaction rate is recovered. In our model the random time interval of n reorientation attempts is given by $T(n) = \sum_{i=1}^{n} T_i$, $T(0) = 0$. Therefore, the simplest way to mimic the experimental procedure is to impose the following conditions on the parameters γ and α (see, Eq. (27)):

$$\gamma = \gamma_1, \quad \alpha = \alpha_1 = (1 + 1/\gamma_1)^{-1}, \quad \text{if} \quad T(n) \leq t_w, \tag{34}$$

$$\gamma = \gamma_2, \quad \alpha = \alpha_2 = (1 + 1/\gamma_2)^{-1}, \quad \text{if} \quad T(n) > t_w. \tag{35}$$

For each independent run, there exists an index n such that $T(n) \leq t_w < T(n+1)$. Consequently, the waiting time $T(n+1) - T(n)$ is extracted from a residence time distribution $\psi(\tau)$ (Eq. (28)) which depends on the parameters γ_1 and α_1. Similarly, the waiting times $T(k+1) - T(k)$ for $k > n$ are determined by the parameters γ_2 and α_2.

Figure 5 shows typical memory effects in our model after an abrupt change of the tapping intensity γ. The simulation data we present therein on the packing fraction $\rho(t)$ are averaged over 10^4 runs. In Figure 5a the tapping intensity γ is switched from $\gamma_1 = 3/2$ ($\alpha_1 = 0.6$) to $\gamma_2 = 3/7$ ($\alpha_2 = 0.3$) at $t_w = 10^4$. We observe that after the transient interval the "anomalous" response ceases and there is a crossover to the "normal" behavior, with compaction rate becoming the same as in the constant forcing mode. In Figure 5b we show the response of the system to the tapping intensity shift from $\gamma_1 = 2/3$ ($\alpha_1 = 0.4$) to $\gamma_2 = 3/2$ ($\alpha_2 = 0.6$) at a time $t_w = 2 \times 10^5$. We observe a memory effect opposite to the previous case, i.e. we find that the system dilates immediately following t_w. Both results are opposite to what could be expected from the long-time behavior at constant γ.

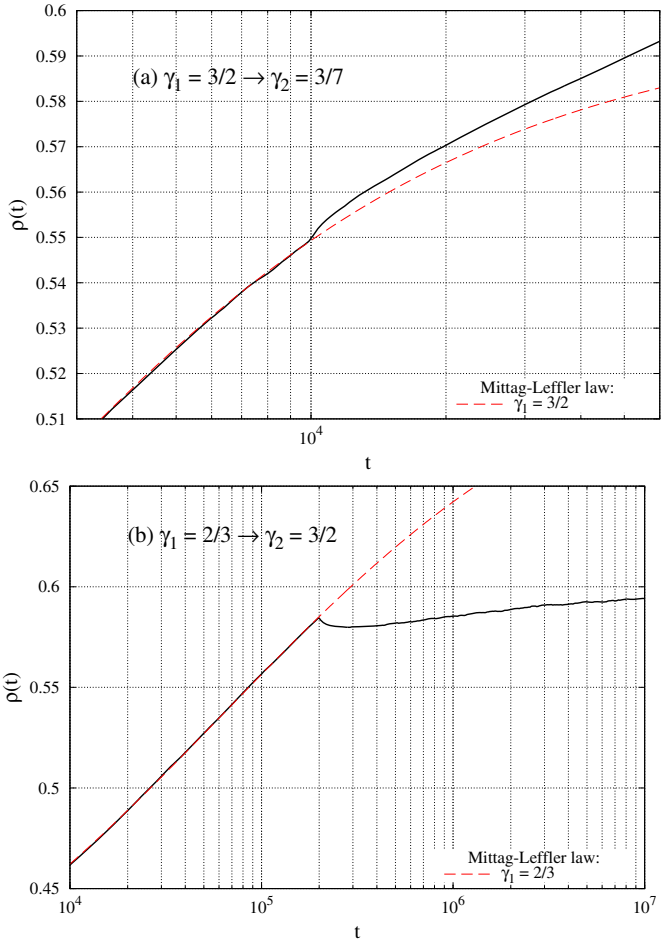

Fig. 5. Memory effects in the present model. Time evolution of the packing fraction $\rho(t)$ when the tapping intensity is switched (a) from $\gamma_1 = 3/2$ to $\gamma_2 = 3/7$ ($\alpha_1 = 0.6 \to \alpha_2 = 0.3$) at $t_w = 10^4$ (upper solid curve), and (b) from $\gamma_1 = 2/3$ to $\gamma_2 = 3/2$ ($\alpha_1 = 0.4 \to \alpha_2 = 0.6$) at $t_w = 2 \times 10^5$ (lower solid curve). The dashed curves obtained analytically by equation (23) correspond to the processes at constant $\gamma_1 = 3/2$ (a), and $\gamma_1 = 2/3$ (b). Simulation results come from an average over 10^4 simulations.

Memory effect implies that the system can be found in states, characterized by the same packing fraction ρ, that evolve differently under further tapping with the same intensity γ. This is illustrated in Figure 6. For the tapping intensities $\gamma = 3/2$ ($\alpha = 0.6$) and $11/9$ ($\alpha = 0.55$) our system achieves the packing fraction $\rho_w = 0.5624$ at the same time $t_w = 1.654 \times 10^4$. First, the system was driven to the same packing fraction ρ_w with two different tapping intensities, $\gamma_1 = 3/2$ and $\gamma_2 = 11/9$. After the packing fraction ρ_w was achieved at time t_w, the system was always tapped with the same intensity, γ_2. The time evolution of the packing fraction is shown in Figure 6a. In the

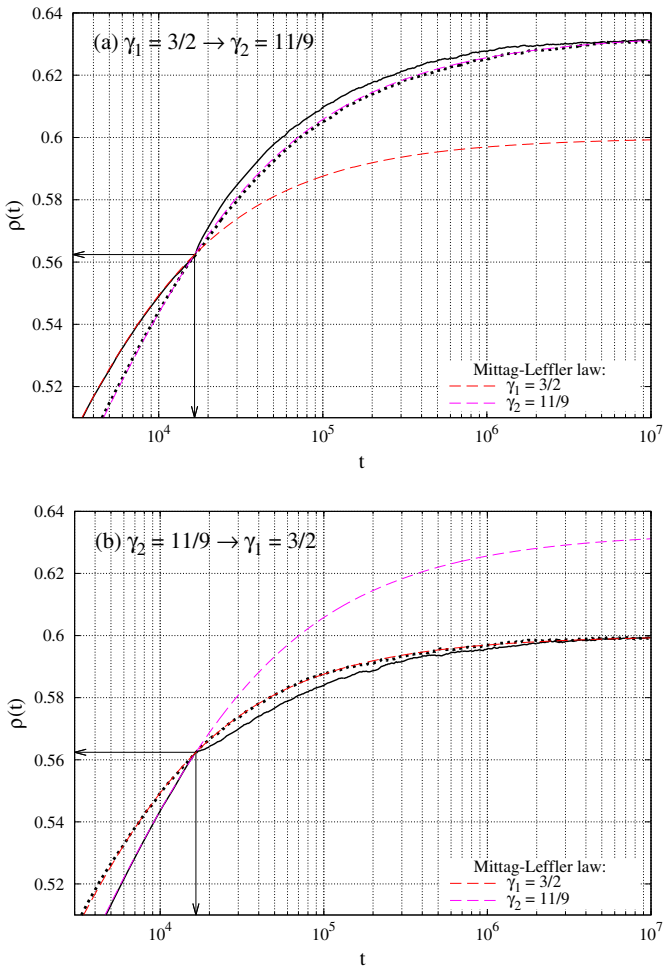

Fig. 6. Time evolution of the packing fraction for a system, which was tapped up to the same packing fraction $\rho_w = 0.5624$ using two different tapping intensities, $\gamma_1 = 3/2$ ($\alpha_1 = 0.6$) and $\gamma_2 = 11/9$ ($\alpha_2 = 0.55$). Afterwards, the system was always tapped with (a) $\gamma_2 = 11/9$, and (b) $\gamma_1 = 3/2$. Solid line presents the results of simulation in which there is a change in the tapping intensity γ at time $t_w = 1.654 \times 10^4$: (a) $\gamma_1 = 3/2 \rightarrow \gamma_2 = 11/9$, and (b) $\gamma_2 = 11/9 \rightarrow \gamma_1 = 3/2$. The curve corresponding to a constant tapping intensity is plotted for reference (dotted line). The dashed curves obtained analytically by equation (23) correspond to a processes at constant $\gamma_1 = 3/2$ and $\gamma_2 = 11/9$. Simulation results come from an average over 10^4 simulations. The evolution for $t > t_w$ depends on the prehistory of the system.

second case, the tapping intensity γ_2 was switched to γ_1 at time t_w (see Fig. 6b). Note that in all the plotted curves the jump of the compaction rate has an opposite sign than the variation of the tapping intensity. Figures 6a and 6b clearly show that the two systems prepared at the same packing fraction but in different ways display different behaviors if the same tapping acceleration is applied to them. In other words, the density after the perturbation of the tapping intensities depends not only on the density ρ_w, but also on the previous tapping history.

4 Final remarks

In this paper, a one-dimensional model for compaction in granular media has been presented. Trying to mimic what is done in real experiments, the evolution of a two-state system was modeled as a stochastic fractional process. The general probabilistic formalism treats the compaction process of a granular system regardless of the precise nature of local interactions. Within our approach we model the compaction dynamics in terms of a suitable waiting-time distribution between the attempted changes of state. The stochastic time clock has a clear physical sense; a grain interacts with a disordered environment in random points of time. The model has shown to share many of the characteristic features of granular materials under tapping. We have derived the empirical relaxation law (Eq. (23)) and its macroscopic equation (Eq. (22)). In particular, we have shown that the generalized relaxation time τ_r can be accurately described by means of the Arrhenius law (33).

The validity of our fractional kinetic approach to the situation when the tapping intensity is abruptly increased or decreased is proved by comparison to numerical simulations of the corresponding system. The numerical simulations confirm that the packing fraction alone is not sufficient to describe the state of the system, because the future evolution of the density depends not only on its current value, but also on the previous tapping history. The linear response of an ensemble of random walkers performing CTRWs to a changing external field has been previously investigated in several works [57–59]. The response depends on the delay between the time of measurement and the time at which the system was prepared in a given state, i.e. the CTRW process displays aging. The behavior of such systems depends much on the early history of the system. It should be noted that the memory effects are a direct consequence of the random time steps τ belonging to the long-tailed waiting-time distribution $\psi(\tau)$ (28). Completely expected, granular compaction is an example of a non-local temporal phenomena in which a different kind of calculus, i.e. fractional calculus, should play a central role.

This work was supported by the Ministry of Education, Science and Technological Development of the Republic of Serbia, under Grant Nos. ON171017 and III45016.

References

1. P. Richard, M. Nicodemi, R. Delannay, P. Ribière, D. Bideau, Nat. Mater. **4**, 121 (2005)
2. J.B. Knight, C.G. Fandrich, C.N. Lau, H.M. Jaeger, S.R. Nagel, Phys. Rev. E **51**, 3957 (1995)
3. F.X. Villarruel, B.E. Lauderdale, D.M. Mueth, H.M. Jaeger, Phys. Rev. E **61**, 6914 (2000)
4. P. Philippe, D. Bideau, Europhys. Lett. **60**, 677 (2002)
5. P. Ribière, P. Richard, D. Bideau, R. Delannay, Eur. Phys. J. E **16**, 415 (2005)
6. P. Ribière, P. Richard, P. Philippe, D. Bideau, R. Delannay, Eur. Phys. J. E **22**, 249 (2007)

7. G. Lumay, N. Vandewalle, Phys. Rev. Lett. **95**, 028002 (2005)
8. G. Lumay, N. Vandewalle, Phys. Rev. E **74**, 021301 (2006)
9. M. Nicolas, P. Duru, O. Pouliquen, Eur. Phys. J. E **3**, 309 (2000)
10. O. Pouliquen, M. Belzons, M. Nicolas, Phys. Rev. Lett. **91**, 014301 (2003)
11. D. Arsenović, S.B. Vrhovac, Z.M. Jakšić, L. Budinski-Petković, A. Belić, Phys. Rev. E **74**, 061302 (2006)
12. S. Živković, Z.M. Jakšić, D. Arsenović, L. Budinski-Petković, S.B. Vrhovac, Granular Matter **13**, 493 (2011)
13. R. Hilfer, J. Non-Cryst. Solids **305**, 122 (2002)
14. Lj. Budinski-Petković, M. Petković, Z.M. Jakšić, S.B. Vrhovac, Phys. Rev. E **72**, 046118 (2005)
15. J. Talbot, G. Tarjus, P. Viot, Phys. Rev. E **61**, 5429 (2000)
16. G. Tarjus, P. Viot, Phys. Rev. E **69**, 011307 (2004)
17. Lj. Budinski-Petković, S.B. Vrhovac, Eur. Phys. J. E **16**, 89 (2005)
18. W.L. Vargas, J.J. McCarthy, Phys. Rev. E **76**, 041301 (2007)
19. T. Divoux, H. Gayvallet, J.-C. Géminard, Phys. Rev. Lett. **101**, 148303 (2008)
20. N. Mueggenburg, Phys. Rev. E **85**, 041305 (2012)
21. A.J. Kolan, E.R. Nowak, A.V. Tkachenko, Phys. Rev. E **59**, 3094 (1999)
22. J. Talbot, G. Tarjus, P. Viot, Eur. Phys. J. E **5**, 445 (2001)
23. M. Nicodemi, A. Coniglio, Phys. Rev. Lett. **82**, 916 (1999)
24. A. Barrat, V. Loreto, J. Phys. A **33**, 4401 (2000)
25. A. Barrat, V. Loreto, Europhys. Lett. **53**, 297 (2001)
26. A. Fierro, M. Nicodemi, A. Coniglio, Phys. Rev. E **66**, 061301 (2002)
27. P.F. Stadler, J.M. Luck, A. Mehta, Eurohys. Lett. **57**, 46 (2001)
28. J.J. Brey, A. Prados, B. Sanchez-Rey, Phys. Rev. E **60**, 5685 (1999)
29. J.J. Brey, A. Prados, Phys. Rev. E **63**, 061301 (2001)
30. A. Prados, J.J. Brey, Phys. Rev. E **66**, 041308 (2002)
31. J.J. Brey, A. Prados, Phys. Rev. E **68**, 051302 (2003)
32. S.F. Edwards, D.V. Grinev, Phys. Rev. E **58**, 4758 (1998)
33. C. Josserand, A. Tkachenko, D.M. Mueth, H.M. Jaeger, Phys. Rev. Lett. **85**, 3632 (2000)
34. L.A. Pugnaloni, G.C. Barker, Physica A **337**, 428 (2004)
35. R. Arévalo, D. Maza, L.A. Pugnaloni, Phys. Rev. E **74**, 021303 (2006)
36. L.A. Pugnaloni, M.G. Valluzzi, L.G. Valluzzi, Phys. Rev. E **73**, 051302 (2006)
37. G. Marty, O. Dauchot, Phys. Rev. Lett. **94**, 015701 (2005)
38. R. Metzler, J. Klafter, Phys. Rep. **339**, 1 (2000)
39. A. Mehta, G.C. Barker, J.M. Luck, J. Stat. Mech.: Theor. Exp. **2004**, P10014 (2004)
40. P. Ribière, P. Richard, R. Delannay, D. Bideau, Phys. Rev. Lett. **95**, 268001 (2005)
41. A. Janicki, A. Weron, Stat. Sci. **9**, 109 (1994)
42. M.M. Meerschaert, H.-P. Scheffler, J. Appl. Probab. **41**, 623 (2004)
43. F. Mainardi, Chaos Solitons Fractals **7**, 1461 (1996)
44. A.A. Stanislavsky, Phys. Rev. E **67**, 021111 (2003)
45. A.A. Stanislavsky, Acta Physica Polonica B **34**, 3649 (2003)
46. F. Mainardi, R. Gorenflo, J. Comput. Appl. Math. **118**, 283 (2000)
47. R.K. Saxena, A.M. Mathai, H.J. Haubold, Physica A **344**, 657 (2004)
48. P. Philippe, D. Bideau, Phys. Rev. Lett. **91**, 104302 (2003)
49. N. Gravish, S.V. Franklin, D.L. Hu, D.I. Goldman, Phys. Rev. Lett. **108**, 208001 (2012)
50. E. Heinsalu, M. Patriarca, I. Goychuk, G. Schmid, P. Hänggi, Phys. Rev. E **73**, 046133 (2006)
51. E. Heinsalu, M. Patriarca, I. Goychuk, P. Hänggi, J. Phys.: Condens. Matter **19**, 065114 (2007)
52. R. Hilfer, L. Anton, Phys. Rev. E **51**, R848 (1995)
53. D. Fulger, E. Scalas, G. Germano, Phys. Rev. E **77**, 021122 (2008)
54. T.J. Kozubowski, S.T. Rachev, Int. J. Comput. Numer. Anal. Appl. **1**, 177 (1999)
55. E.R. Nowak, J.B. Knight, M.L. Povinelli, H.M. Jaeger, S.R. Nagel, Powder Technol. **94**, 79 (1997)
56. E.R. Nowak, J.B. Knight, E. Ben-Naim, H.M. Jaeger, S.R. Nagel, Phys. Rev. E **57**, 1971 (1998)
57. I.M. Sokolov, A. Blumen, J. Klafter, Europhys. Lett. **56**, 175 (2001)
58. I.M. Sokolov, A. Blumen, J. Klafter, Physica A **302**, 268 (2001)
59. I.M. Sokolov, Phys. Rev. E **73**, 067102 (2006)